

## ■ Scandium Complexes

# Reduced Arene Complexes of Scandium

Priyabrata Ghana, Alexander Hoffmann, Thomas P. Spaniol, and Jun Okuda\*<sup>[a]</sup>

**Abstract:** Alkali metal naphthalenide or anthracenide reacted with scandium(III) anilides  $[\text{Sc}(\text{X})\{\text{N}(\text{tBu})\text{Xy}\}_2(\text{thf})]$  ( $\text{X} = \text{N}(\text{tBu})\text{Xy}$  (**1**);  $\text{X} = \text{Cl}$  (**2**);  $\text{Xy} = \text{C}_6\text{H}_3\text{-}3,5\text{-Me}_2$ ) to give scandium complexes  $[\text{M}(\text{thf})_n][\text{Sc}\{\text{N}(\text{tBu})\text{Xy}\}_2(\text{RA})]$  ( $\text{M} = \text{Li-K}$ ;  $n = 1-6$ ;  $\text{RA} = \text{C}_{10}\text{H}_8^{2-}$  (**3-Naph-K**) and  $\text{C}_{14}\text{H}_{10}^{2-}$  (**3-Anth-M**)) containing a reduced arene ligand. Single-crystal X-ray diffraction revealed the scandium(III) center bonded to the naphthalene dianion in a  $\sigma^2:\pi$ -coordination mode, whereas the anthracene dianion is symmetrically attached to the scandium(III) center in a  $\sigma^2$ -fashion. All compounds have been character-

ized by multinuclear, including  $^{45}\text{Sc}$  NMR spectroscopy. Quantum chemical calculations of these intensely colored arene complexes confirm scandium to be in the oxidation state +3. The intense absorptions observed in the UV/Vis spectra are due to ligand-to-metal charge transfers. Whereas nitriles underwent C–C coupling reaction with the reduced arene ligand, the reaction with one equivalent of  $[\text{NEt}_3\text{H}][\text{BPh}_4]$  led to the mono-protonation of the reduced arene ligand.

## Introduction

Complexes of alkali and alkaline earth metals with mono- or dianionic naphthalene<sup>[1]</sup> and anthracene<sup>[2]</sup> ligands are used as strong reductants for the synthesis of low-valent organometallic and main-group compounds as well as for highly pure metal nanoparticles.<sup>[3]</sup> Bonding in this class of compounds ranges from strong  $\sigma$  bonds to weak electrostatic interactions and involves varied coordination numbers.<sup>[4]</sup> Metal complexes with dianionic, conjugated benzenoid polycyclic ligands have also been used to probe the concept of aromaticity and antiaromaticity.<sup>[5]</sup> However, only few examples of transition-metal complexes with dianionic naphthalene and anthracene ligands have been described,<sup>[6]</sup> their applications in synthetic chemistry still being limited. Recently, some of these highly reduced transition-metal complexes were reported to activate small molecules or to serve as synthons for reduced metal fragments.<sup>[6e,g,7a,b]</sup> Only few related lanthanide complexes are known.<sup>[4b,8a-e]</sup> Scandium combines properties of main-group elements, transition metals, and lanthanides. The first scandium(III) complex with a reduced arene ligand was synthesized in 2011, when Diaconescu et al. reported the naphthalene derivative  $[(\text{NN}^{\text{fc}})\text{Sc}]_2(\mu\text{-C}_{10}\text{H}_8)$  ( $\text{NN}^{\text{fc}} = (\text{NSi}^{\text{tBu}}\text{Me}_2)_2\text{fc}$ ;  $\text{fc} = 1,1'$ -ferrocene-

nediyl) and the anthracene derivative  $[(\text{NN}^{\text{fc}})\text{Sc}]_2(\mu\text{-C}_{14}\text{H}_{10})$ .<sup>[9]</sup> It was suggested that both complexes are stabilized through the interaction of the scandium centers with the ferrocene backbone.<sup>[9]</sup> A similar mono-scandium reduced naphthalene complex  $[\text{K}\{(\text{NN}^{\text{fc}})\text{Sc}\}(\mu\text{-C}_{10}\text{H}_8)]$  was also proposed to form in solution, but due to thermal instability no spectroscopic or structural data were given.<sup>[10]</sup> So far, there are no reports on any isolable mononuclear scandium complex of reduced arenes.<sup>[11]</sup> Taking advantage of the bulky anilide ligand  $\text{N}(\text{tBu})(\text{Xy})$  ( $\text{Xy} = \text{C}_6\text{H}_3\text{-}3,5\text{-Me}_2$ : “Cummin’s ligand”), which has provided access to many unusually reactive metal complexes in the past,<sup>[12]</sup> we present here a series of isolable mono-scandium complexes of reduced naphthalene and anthracene ligands.

## Results and Discussion

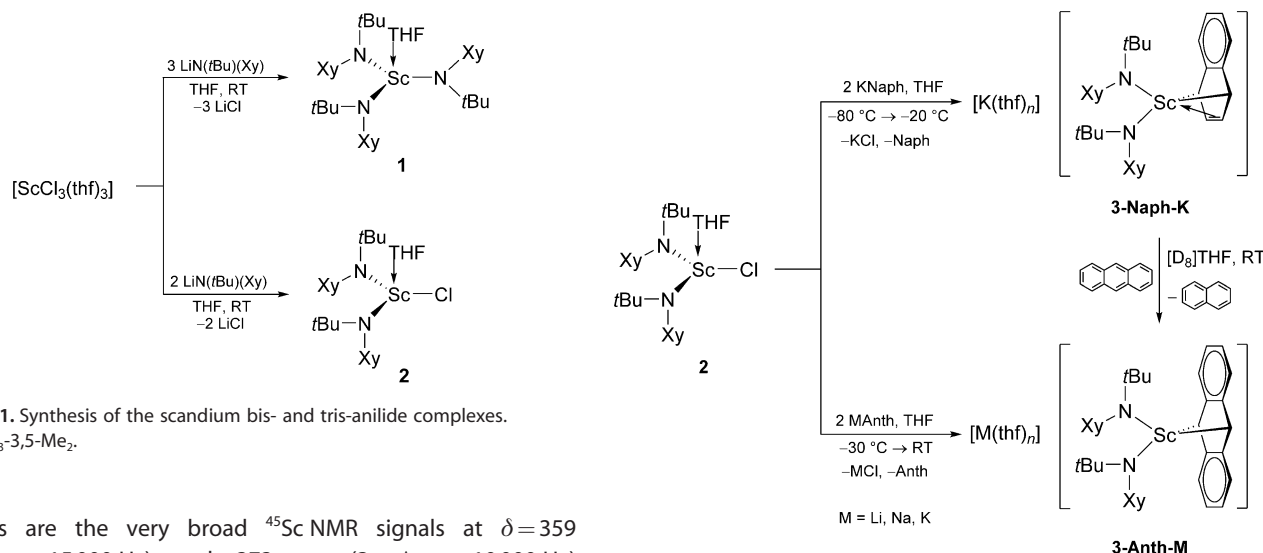
The tris- or bis-anilide complexes  $[\text{Sc}\{\text{N}(\text{Xy})(\text{tBu})\}_3(\text{thf})]$  (**1**) and  $[\text{ScCl}\{\text{N}(\text{Xy})(\text{tBu})\}_2(\text{thf})]$  (**2**), were prepared in THF at ambient temperature by reacting the THF adduct of scandium trichloride,  $[\text{ScCl}_3(\text{thf})_3]$ , with three or two equiv of  $\text{LiN}(\text{tBu})\text{Xy}$ , respectively (Scheme 1). Both complexes were isolated in moderate to good yield (**1**: 82%; **2**: 51%) as colorless solids (see the Supporting Information, Sections 2.1 and 2.2). Both compounds are stable in the solid state if air is completely excluded. At ambient temperature, **2** slowly disproportionates in solution to give **1** and  $[\text{ScCl}_2\{\text{N}(\text{Xy})(\text{tBu})\}(\text{thf})]$ , as observed by  $^1\text{H}$  NMR spectroscopy.

In the solid state, compounds **1** and **2** contain four-coordinate scandium centers in distorted tetrahedral geometry (Figures S36 and S37 in the Supporting Information).<sup>[13]</sup> The larger sum of the angles between the three anilide ligands in **1** ( $343.8^\circ$ ) than the angle sum between the anilide and chloride ligands in **2** ( $326.2^\circ$ ) reveals a lower degree of pyramidalization of 18% in **1** (compared to 38% in **2**).<sup>[14]</sup> Notable spectroscopic

[a] Dr. P. Ghana, Dr. A. Hoffmann, Dr. T. P. Spaniol, Prof. Dr. J. Okuda  
Institute of Inorganic Chemistry, RWTH Aachen University  
Landoltweg 1, 52056 Aachen (Germany)  
E-mail: jun.okuda@ac.rwth-aachen.de

Supporting information and the ORCID identification number(s) for the author(s) of this article can be found under:  
<https://doi.org/10.1002/chem.202000946>.

© 2020 The Authors. Published by Wiley-VCH Verlag GmbH & Co. KGaA. This is an open access article under the terms of Creative Commons Attribution NonCommercial-NoDerivs License, which permits use and distribution in any medium, provided the original work is properly cited, the use is non-commercial and no modifications or adaptations are made.



**Scheme 1.** Synthesis of the scandium bis- and tris-anilide complexes.  $Xy = C_6H_3-3,5-Me_2$ .

features are the very broad  $^{45}Sc$  NMR signals at  $\delta = 359$  (**1**,  $\Delta\nu_{1/2} = 15000$  Hz) and 373 ppm (**2**,  $\Delta\nu_{1/2} = 10000$  Hz) (Figure 2), close to that of the homoleptic tris(amide) complex  $[Sc\{N(SiMe_3)_2\}_3]$  ( $\delta(^{45}Sc) = 396$  ppm).<sup>[15]</sup> The high-field shift is likely caused by the higher coordination number (four vs. three) of the scandium centers in **1** and **2**.<sup>[15]</sup>

Reduction of **1** with two equivalents of potassium naphthalenide (KNaph) in THF at low temperature led to a color change of the mixture from colorless to dark purple. Monitoring the reaction by variable-temperature (VT)  $^1H$  NMR spectroscopy revealed that the reaction proceeded smoothly to form a thermolabile, diamagnetic complex  $[K(thf)_n][Sc\{N(tBu)(Xy)\}_2(Naph)]$  (**3-Naph-K**) along with  $[KN(tBu)(Xy)]$  at around  $-30$  to  $-20^\circ C$  (Figure S11). Warming the dark-purple solution to room temperature led to decomposition. Workup and fractional crystallization at  $-60^\circ C$  allowed the isolation of **3-Naph-K** as dark-purple crystals in 26% yield (see the Supporting Information, Section 2.3). The compound is highly air sensitive and decolorizes instantaneously upon exposure to air. **3-Naph-K** was isolated in 64% yield when the chloro complex **2** was used instead of **1**, whereby KCl is formed instead of the ionic potassium anilide  $[KN(tBu)(Xy)]$  which cannot easily be separated from the main product (Scheme 2). When the reduction of **2** was carried out in one pot by mixing **2**, naphthalene, and  $KC_8$  in a 1:1:2 or in a 1:2:2 ratio, the formation of **3-Naph-K** was also observed as the major product. However, due to the formation of an unknown side product, this method was unsuitable for large-scale synthesis. Whereas the bulky anilide ligand  $N(tBu)(Xy)$  allowed to stabilize the arene complex **3-Naph-K**, reduction of the scandium bis(trimethylsilyl)amide iodide  $[(Me_3Si)_2N]_2ScI(thf)$  by using a mixture of  $KC_8$  and naphthalene did not provide a reduced naphthalene complex.<sup>[9]</sup>

To understand the mechanism of the formation of **3-Naph-K**, the reduction of complexes **1** and **2** with KNaph was tried with different stoichiometry. When complex **1** or **2** was reduced with one equivalent of KNaph at  $-80^\circ C$  and slowly brought to room temperature, formation of a 1:1:1 mixture of **3-Naph-K**, free naphthalene, and **1** or **2** was observed. This indicates that the reduction of **1** or **2** with one equivalent of KNaph probably leads to the formation of an unstable paramagnetic intermediate  $[Sc\{N(tBu)(Xy)\}_2](thf)_n$ , which instantane-

**Scheme 2.** Synthesis of the reduced arene complexes of scandium.

ously reacts with another equivalent of KNaph to form **3-Naph-K**. To support this proposed mechanism, the reaction of **1** with two equivalents of KNaph was followed by VT NMR spectroscopy (Figure S11), which shows the formation of only **3-Naph-K** and  $[KN(tBu)(Xy)]$  without any other intermediates. In addition to VT NMR spectroscopy, the reduction of **2** was also tested in the absence of naphthalene by using one equivalent of  $KC_8$  as reductant. This reaction led to an untraceable mixture of products.

The solid-state structure of the solvate **3-Naph-K**·THF was determined by X-ray diffraction and revealed a contact ion pair with the potassium cation located within a pocket formed by three THF molecules, one amide ligand, and the aromatic ring of the naphthalene ligand (Figure 1). The only other known scandium complex of reduced naphthalene shows an inverted sandwich structure with two metal centers and one naphthalene ligand, which is the common structural pattern observed for most reduced arene complexes of the rare earth metals.<sup>[4b]</sup> The molecular structure reveals a  $\sigma^2:\pi$ -coordinated arene ligand with Sc–C1/C4 distances of 2.355(4) and 2.322(3) Å, as well as Sc–C2/C3 distances of 2.448(4) and 2.475(3) Å, respectively. A similar  $\sigma^2:\pi$ -coordination was also observed in an yttrium reduced naphthalene complex  $[K(2.2.2\text{-cryptand})][Cp'_2Y(\eta^4-C_{10}H_8)]$  ( $Cp' = C_5H_4SiMe_3$ ).<sup>[16]</sup> In addition to the strong coordination to scandium, the resulting  $sp^3$  hybridization of the C1 and C4 atoms is expressed by a large folding angle of  $35.63(19)^\circ$  between the planes defined by C1–C2–C3–C4 and C1–C9–C10–C4. This deviation from planarity is more pronounced than that in the previously reported scandium naphthalene complex  $[(NN^tC)Sc]_2(\mu-C_{10}H_8)$ , where the corresponding folding angle is around  $18^\circ$  and where the Sc–C(naphthalene) distances of  $d(Sc-C)_{avg} = 2.514$  Å<sup>[9]</sup> are not as short as in **3-Naph-K**. The alternating bond lengths C1–C2 (1.458(6) Å), C2–C3 (1.349(5) Å), and C3–C4 (1.452(5) Å) also indicate a  $\sigma^2:\pi$ -canonical rather than a  $\pi^2$ -canonical structure. The strong electron donation of the naphthalene dianion explains the longer Sc–N bonds

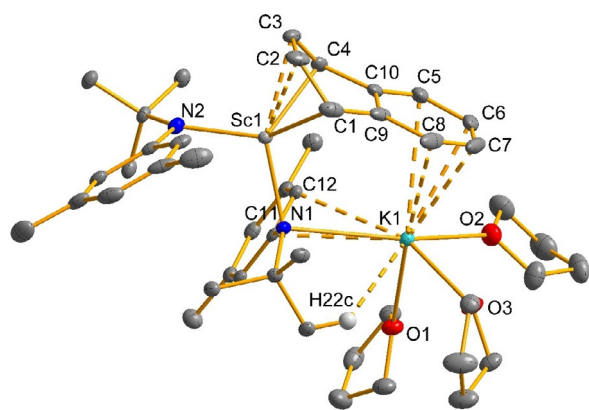


**Figure 1.** Molecular structure of one of the crystallographically independent molecules of **3-Naph-K** in the solid state with displacement parameters at 30% probability level. Hydrogen atoms except for H22c are omitted for clarity. Selected interatomic distances (Å) and angles (°): Sc1–N1 2.181(3), Sc1–N2 2.135(3), Sc1–C1 2.355(4), Sc1–C2 2.488(4), Sc1–C3 2.475(3), Sc1–C4 2.322(3), K1–N1 3.065(3), K1–O1 2.669(2), K1–O2 2.737(3), K1–O3 2.695(3), K1–C5 3.426(4), K1–C6 3.126(4), K1–C7 3.017(5), K1–C8 3.222(5); N1–Sc1–N2 107.93(10), C1–Sc1–C4 72.51(14), N1–K1–O2 153.68(8).

( $d(\text{Sc}-\text{N}1)=2.181(3)$  Å;  $d(\text{Sc}-\text{N}2)=2.135(3)$  Å) than in the precursors **1** ( $d(\text{Sc}-\text{N})_{\text{avg}}=2.064$  Å) or **2** ( $d(\text{Sc}-\text{N})_{\text{avg}}=2.037$  Å), most likely due to a significantly decreased N→Sc  $\pi$ -donation in **3-Naph-K**. The K1–N1 distance of 3.065(3) Å is similar to that observed in potassium complexes of diaza-18-crown-6.<sup>[6a,17,13c]</sup> The potassium atom is coordinated by three THF ligands and the naphthalene ring (C5–C8). Additional interactions with the anilide nitrogen atom N1, the carbon atoms C11 and C12 as well as by one hydrogen atom of a methyl group lead to formal coordination number eight.

The structure is maintained in solution, as shown by the  $^1\text{H}$  and  $^{13}\text{C}$  NMR signals for the anilide (N(tBu)Xy) and naphthalene ligands in 2:1 ratio, along with those of coordinated THF. Most characteristic in the  $^1\text{H}$  NMR spectrum are the four naphthalene  $^1\text{H}$  NMR resonances at  $\delta=3.40$  (C<sup>1,4</sup>-H), 4.13 (C<sup>2,3</sup>-H), 5.78 and 6.18 ppm (C<sup>5,8</sup>-H and C<sup>6,7</sup>-H), at considerably higher field than in free naphthalene ( $\delta=7.45$  and 7.84 ppm, in  $[\text{D}_8]\text{THF}$ ). Such an upfield shift is common for metal complexes of reduced naphthalene.<sup>[6f,g,7a,9]</sup> The  $^1\text{H}$  NMR spectrum at  $-20^\circ\text{C}$  is similar to that at room temperature, except for broader *ortho*- and *para*-CH signals of the 3,5-xylyl groups (Figure S8), which indicate hindered rotation of the 3,5-xylyl group around the *ipso*-C–N bond at lower temperatures. The  $^{45}\text{Sc}$  NMR spectrum of **3-Naph-K** in  $[\text{D}_8]\text{THF}$  at room temperature displays a very broad signal due to the quadrupole moment of scandium at  $\delta=364$  ppm with  $\Delta\nu_{1/2}=20\,000$  Hz (Figure 2). Reduction of precursor **1** or **2** with potassium naphthalenide does not affect the  $^{45}\text{Sc}$  shift. Replacing the naphthalenide against the anthracenide ligand had no effect on the chemical shift of the  $^{45}\text{Sc}$  NMR signal (Figure 2). Considering that the  $^{45}\text{Sc}$  resonances highly depend on the coordination number of the scandium center,<sup>[15]</sup> the almost equal  $^{45}\text{Sc}$  chemical shift in **1**, **2**, and **3-Naph-K** indicate that the metal center in the reduced compound is four-coordinate, whereby the weak interactions from the peripheral C=C bonds have only a small effect.

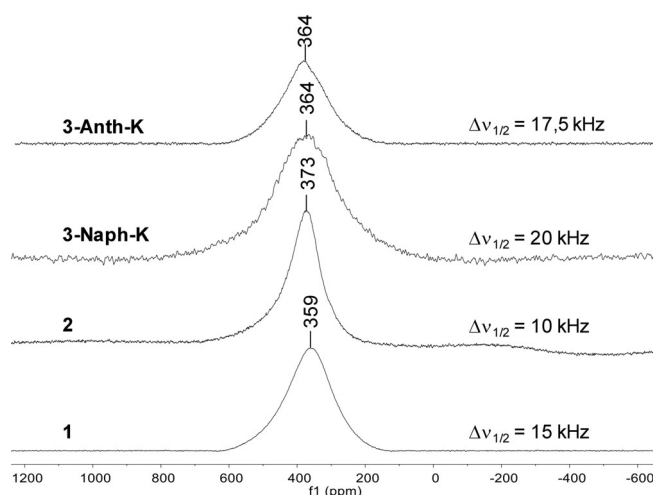


**Figure 2.**  $^{45}\text{Sc}$  NMR spectra of **1**, **2**, **3-Naph-K**, and **3-Anth-K** at room temperature. Line broadening (lb) values are set to 100 Hz.

Treating a 1:1 mixture of **3-Naph-K** and free anthracene in  $[\text{D}_8]\text{THF}$  at ambient temperature led to a color change of the solution from dark-purple to dark-red within 10 min. Inspection of the resulting solution by  $^1\text{H}$  NMR spectroscopy confirmed the complete consumption of **3-Naph-K**. Free naphthalene was formed in addition to the diamagnetic complex  $[\text{K}(\text{thf})][\text{Sc}\{\text{N}(\text{tBu})(\text{Xy})\}_2(\text{Anth})]$  (**3-Anth-K**) that contains a reduced anthracene ligand. This compound was also prepared directly by the reduction of **2** with two equivalents of potassium anthracenide (KAnth) (Scheme 2). Addition of a dark-blue solution of KAnth in THF to a colorless solution of **2** in THF at  $-30^\circ\text{C}$  and warming up the blue solution to room temperature gave **3-Anth-K**, which was isolated as dark-red crystals in 74% yield (see the Supporting Information, Section 2.6). To determine the influence of other alkali metals on the coordination sphere of reduced scandium anthracene complexes, the corresponding Li and Na complexes  $[\text{Li}(\text{thf})_3][\text{Sc}\{\text{N}(\text{tBu})(\text{Xy})\}_2(\text{Anth})]$  (**3-Anth-Li**) and  $[\text{Na}(\text{thf})_4][\text{Sc}\{\text{N}(\text{tBu})(\text{Xy})\}_2(\text{Anth})]$  (**3-Anth-Na**) were prepared in a similar manner and isolated as dark-red, crystalline solids in moderate to good yield (**3-Anth-Li**: 46%, **3-Anth-Na**: 62%) (see the Supporting Information, Sections 2.4 and 2.5). Compounds **3-Anth-M** (M=Li, Na and K) are also thermally unstable, but decompose more slowly at room temperature than **3-Naph-K**. All of these reduced anthracene complexes are highly sensitive towards air where they decolorize instantaneously.

Because of the  $d^0$  configuration of the scandium(III) center, the intense color of all reduced naphthalene and anthracene complexes are notable. UV/Vis spectra of **3-Naph-K** and **3-Anth-K** were recorded at  $-40^\circ\text{C}$  in THF at varied concentrations ( $\approx 8$ – $0.5$  mmol) (Figures S12 and S24). For **3-Naph-K**, a very intense band with an absorption maximum at  $\lambda_{\text{max}}=536$  nm corresponds to the intense purple color of this complex. The UV/Vis spectrum of **3-Anth-K** shows an intense band at  $\lambda_{\text{max}}=462$  nm, corresponding to the intense red color of this anthracene complex. The optical spectra of **3-Anth<sup>-</sup>** and **3-Naph-K** were calculated by using time-dependent DFT and fit well with the experimental spectra (Figure S47). To identify the

nature of the optical transitions, natural transition orbital calculations were performed for the major electronic transitions in both systems (Figure S45 and S46).<sup>[18]</sup> The transitions at higher wavelengths are ligand-to-metal charge transfer transitions (LMCTs) from the reduced anthracene or the naphthalene ligand to the d orbitals of scandium, whereas the transitions at shorter wavelengths correspond to the LMCTs from the amide unit.

According to X-ray diffraction studies, the bonding between the anthracene and the scandium center is similar for all **3-Anth-M** (M=Li, Na, and K) systems, but the overall structure depends on the alkali metal. The potassium cation in **3-Anth-K** forms a contact ion pair (CIP) by coordinating to the anthracene ligand from the opposite direction of the scandium center, but solvent-separated ion pairs (SSIPs) are formed with the lithium and the sodium cations in **3-Anth-Li** and **3-Anth-Na**, respectively (Figures 3 and S39). As expected, the lithium and sodium cations are tetrahedrally and octahedrally coordinated by four and six THF molecules, respectively. These structures differ markedly from that of the previously reported scandium anthracene complex  $[(\text{NN}^{\text{C}})\text{Sc}]_2(\mu\text{-C}_{14}\text{H}_{10})$ , where the two scandium centers are unsymmetrically attached to the anthracene ligand from two opposite directions.<sup>[9]</sup> Bond parameters of **3-Anth-M** confirm that the formally dianionic anthracene is coordinated to the Sc<sup>III</sup> center in  $\sigma^2$ -fashion with weak interactions between the peripheral C=C bonds of the central ring and the scandium center. The  $\sigma$  coordination by the formally sp<sup>3</sup>-hybridized C9 and C10 atoms of the anthracene ring to the metal center is evident by the loss of planarity of the coordinated ring, reflected by large folding angles of around

35.1(2)–38.69(8)°. The Sc–C9/10  $\sigma$ -bond lengths range between 2.3308(16) and 2.358(3) Å and compare with those of the naphthalene complex **3-Naph-K**, but appear shorter than those observed in the scandium anthracene complex  $[(\text{NN}^{\text{C}})\text{Sc}]_2(\mu\text{-C}_{14}\text{H}_{10})$ , where the shortest Sc–C distance observed was 2.442(3) Å.<sup>[9]</sup> Unlike in **3-Naph-K**, where the distances from scandium to the peripheral carbon atoms of the naphthalene ring are rather short (Sc–C2/C3 distances: 2.488(4) and 2.475(3) Å, respectively), the distances from scandium to the peripheral C=C bonds in **3-Anth-M** are much longer and appear in the range of 2.6899(17)–2.7853(15) Å, which are also longer than the average distance observed in the  $\eta^4$ -coordinated scandium complex  $[(\text{NN}^{\text{C}})\text{Sc}]_2(\mu\text{-C}_{14}\text{H}_{10})$  ( $d(\text{Sc}-\text{C}_{\text{C}-\text{C}})_{\text{avg}} = 2.613$  Å).<sup>[9]</sup> This indicates that the anthracene dianion in **3-Anth-M** is formally binding in  $\eta^2$ -fashion to the metal centers through the carbon atoms C9 and C10.

The <sup>1</sup>H and <sup>13</sup>C NMR spectra of the anthracene complexes **3-Anth-M** (M=Li, Na, and K) in [D<sub>6</sub>]THF display three characteristic, highly upfield shifted signals for the anthracene ring proton, among which C<sup>9/10</sup>-H at  $\delta = 3.76$  (**3-Anth-Li**), 3.80 (**3-Anth-Na**), and 3.77 ppm (**3-Anth-K**) are most characteristic, as well as four resonances for the ring carbon atoms, indicating symmetric structures in solution. In the <sup>13</sup>C NMR spectra, the C<sup>9,10</sup> resonances appear at  $\delta = 73.0$  (**3-Anth-Li**), 73.1 (**3-Anth-Na**), and 72.4 ppm (**3-Anth-K**). Such an upfield shift of the anthracene resonances is common for transition-metal complexes of reduced anthracene.<sup>[69,9]</sup> As for **3-Naph-K**, the <sup>45</sup>Sc NMR spectrum of **3-Anth-K** at room temperature displays a very broad signal at  $\delta = 364$  ppm with a line width of  $\Delta\nu_{1/2} = 17500$  Hz (Figure 2). The <sup>7</sup>Li NMR spectrum of **3-Anth-Li** shows

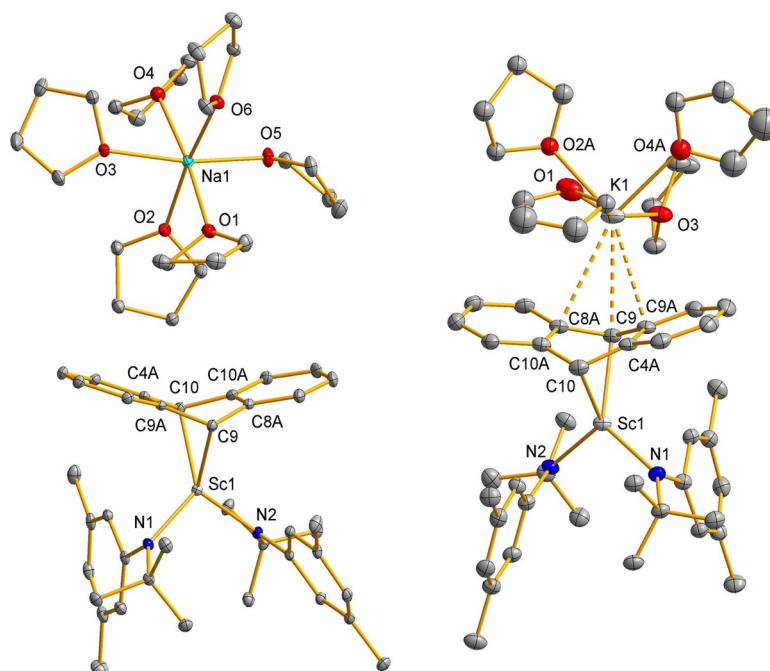


**Figure 3.** Molecular structures of **3-Anth-Na** (left) and one of the two crystallographically independent molecules of **3-Anth-K** (right) in the solid state with displacement parameters at 30% probability level. Hydrogen atoms are omitted for clarity. Selected interatomic distances (Å) and angles (°): **3-Anth-Na**: Sc1–N1 2.1070(14), Sc1–N2 2.1312(12), Sc1–C9 2.3308(16), Sc1–C10 2.3443(16), Sc1–C4A 2.7853(15), Sc1–C8A 2.6929(18), Sc1–C9A 2.7787(15), Sc1–C10A 2.6899(17), N1–Sc1–N2 106.78(5); **3-Anth-K**: Sc1–N1 2.099(4), Sc1–N2 2.101(4), Sc1–C9 2.355(4), Sc1–C10 2.344(5), Sc1–C4A 2.754(5), Sc1–C8A 2.760(5), Sc1–C9A 2.764(5), Sc1–C10A 2.736(5), K1–C8A 3.186(5), K1–C9 3.075(4), K1–C9A 3.136(5), N1–Sc1–N2 108.73(16), Sc2–N3 2.107(4), Sc2–N4 2.106(4).

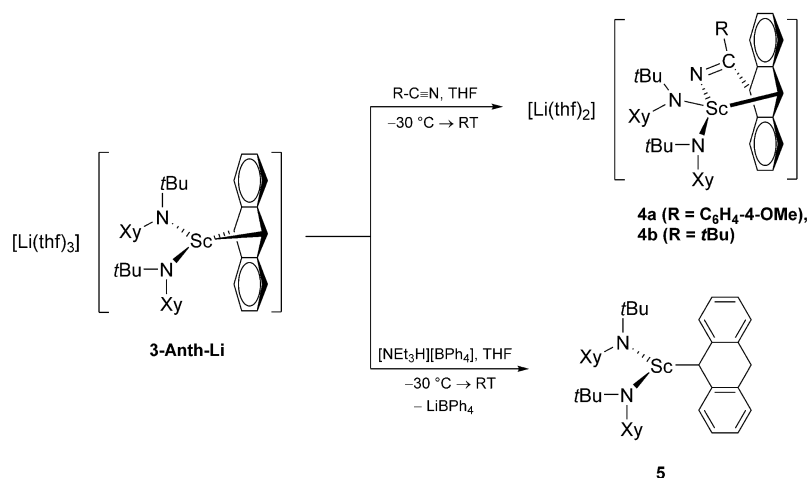
a characteristic signal for tetrahedrally coordinated lithium ion at  $\delta = 0.25$  ppm and the  $^{23}\text{Na}$  NMR spectrum of **3-Anth-Na** shows a broad signal for octahedrally coordinated sodium ion at  $\delta = 7.6$  ppm.

To obtain further insight into the bonding situation, we performed density functional theory (DFT) calculations at the TPSSh-D3/def2-TZVP level of theory.<sup>[19]</sup> For the contact ion pair **3-Naph-K** and the anion **3-Anth<sup>-</sup>**, the singlet and triplet states were calculated to investigate the bonding situation. In both complexes, the singlet state was found to be the lowest in energy (see Table S4); consequently, the scandium ion possesses oxidation state +III and naphthalene or anthracene are dianionic ligands. Key geometric parameters of both structures are summarized in Tables S5 and S6 and the calculated structures agree with the structures obtained by single-crystal X-ray diffraction. The character of the bonds around the scandium ions was evaluated by using the Wiberg bond indices (WBI, Table S7), as well as with the natural bond orbital (NBO) analysis (NBO charges and charge-transfer energies, Table S8).<sup>[20]</sup> The Sc–N bonds (WBI of 0.42 and 0.52 in **3-Naph-K** and 0.46 in **3-Anth<sup>-</sup>**) as well as the short Sc–C<sub>naph</sub> bonds in **3-Naph-K** (WBI of 0.40 and 0.44) and the short Sc–C<sub>anth</sub> bonds in **3-Anth<sup>-</sup>** (WBI of 0.37) show a weakly covalent character. The other Sc–C<sub>naph</sub> or the Sc–C<sub>anth</sub> bonds show only a weak interaction (WBI of 0.21 and 0.22 in **3-Naph-K** and 0.09 and 0.10 in **3-Anth<sup>-</sup>**). The NBO charge of the scandium is +1.4 e<sup>-</sup> in **3-Naph-K** and +1.6 e<sup>-</sup> in **3-Anth<sup>-</sup>**. The higher electronegativity of the N donor atoms results in a more negative NBO charge (–0.75 to –0.77 e<sup>-</sup> units) in comparison to the carbon atoms coordinated to the Sc center with the shorter bond lengths possess a much more negative charge than the carbon atoms with the longer Sc–C bond length, like in other scandium arene complexes.<sup>[9]</sup> For both complexes, two lone pairs of each N atom show charge-transfer donations to the Sc atom (see Table S7). One lone pair possesses p character and the second lone pair sp<sup>2</sup> character (see Table S8 and Figure S48). The charge transfer of both types of lone pairs of the N atoms to the Sc atoms are in the same range comparing between the two compounds (lone

pair with sp<sup>2</sup> character: **3-Naph-K**: 40.1 and 45.6 kcal mol<sup>-1</sup>; **3-Anth<sup>-</sup>**: 39.4 and 43.3 kcal mol<sup>-1</sup> or lone pair with p character **3-Naph-K**: 10.0 and 11.7 kcal mol<sup>-1</sup>; **3-Anth<sup>-</sup>**: 10.7 and 12.8 kcal mol<sup>-1</sup>). So, the donor–acceptor interactions show additional ionic character. For the bonded C atoms of the anthracene or naphthalene moiety no donor–acceptor interaction to the scandium atom could be derived due to the covalent character of the bond (see Figure S49). The NBO analysis describes these bonds as being polarized with strong localization on the corresponding carbon atoms (Table S9, **3-Naph-K**: 13.9 and 15.3% on Sc; 86.1 and 84.7% on C for the corresponding Sc–C bonds; **3-Anth<sup>-</sup>**: 12.6 and 12.5% on Sc; 87.4 or 87.6% on C for the corresponding Sc–C bonds).

Addition of one equiv of 4-methoxybenzotrile or *tert*-butyl nitrile to a dark-red solution of **3-Anth-Li** at –30 °C was accompanied by a rapid color change to reddish brown or greenish yellow, respectively. Inspection of the crude reaction mixture by <sup>1</sup>H NMR spectroscopy indicated the formation of [Li(thf)<sub>n</sub>][Sc{N(*t*Bu)Xy}<sub>2</sub>(Anth)(R–C=N)] (R = C<sub>6</sub>H<sub>4</sub>-4-OMe (**4a**); R = *t*Bu (**4b**); *n* = 0–2) (Scheme 3), which were isolated as pure solids in good yield (brick red, 75% (**4a**); bright yellow, 90% (**4b**)). Unlike the starting anthracene complex, both complexes are thermally stable but decompose immediately upon exposure to air.

The molecular structures of **4a** and **4b** as determined by single-crystal X-ray diffraction show four-coordinate scandium centers in a distorted tetrahedral geometry within a bicyclic ScC<sub>5</sub>N ring (Figure 4, S42, and S43). Although the geometry around the scandium centers is similar in both complexes, the coordination mode of lithium is different. Whereas complex **4a** forms a solvent-separated ion pair with lithium being coordinated by four THF molecules, complex **4b** is a contact ion pair with lithium being bonded to one THF molecule, two nitrogen atoms of an anilide, and the imine groups. The Sc–C<sub>Anth</sub> bond lengths of both complexes are similar (2.348(4) (**4a**) and 2.323(3) Å (**4b**)) and compare with the starting material **3-Anth-Li** (2.358(3) Å). Upon insertion, the C–N bond of the nitriles was elongated significantly (1.259(5) (**4a**), 1.264(4) vs. 1.1516(16) Å (4-methoxybenzotrile)),<sup>[21]</sup> indicating the forma-



**Scheme 3.** Reaction of **3-Anth-Li** with nitriles and [NEt<sub>3</sub>H][BPh<sub>4</sub>].

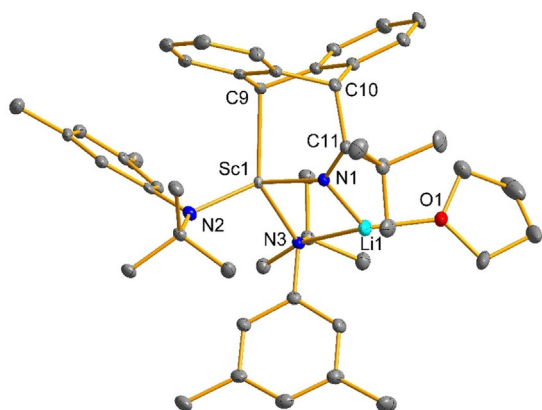


**Figure 4.** Molecular structure of **4b** in the solid state with displacement parameters at 30% probability level. Hydrogen atoms are omitted for clarity. Selected interatomic distances (Å) and angles (°): Sc1–N1 2.062(2), Sc1–N2 2.090(3), Sc1–N3 2.155(2), Sc1–C9 2.323(3), Sc–C10 2.348(4), N1–C11 1.264(4), C10–C11 1.553(4), Li1–N1 1.952(6), Li1–N3 2.140(6), Li1–O1 1.924(6); N1–Sc1–N2 110.80(10), N1–Sc1–N3 90.97(9), N2–Sc1–N3 112.11(10), C9–Sc1–N1 91.21(10), C9–Sc1–N2 115.22(10), C9–Sc1–N3 128.17(11).

tion of an iminyl anion ( $R_2C=N^-$ ) after C–C coupling with the anthracene ligand. A similar C–C coupling reaction was previously observed for the insertion of benzonitrile into the Sc–C bond of a scandium butadiene complex.<sup>[22]</sup> Notably, the reduction of nitriles with alkali metal anthracenides generally leads to decyanation of the nitriles, and C–C coupling of the reduced nitrile group was only observed as a side reaction in a minor quantity.<sup>[23]</sup>

Compounds **4a** and **4b** have also been characterized by  $^1H$ ,  $^{13}C$ ,  $^7Li$ , and  $^{45}Sc$  NMR spectroscopy, which confirm the overall  $C_s$  symmetry of the complexes in solution. As expected, in the  $^1H$  and  $^{13}C$  NMR spectra the C9 and C10 atoms of the anthracene and the corresponding protons appear at high field (see the Supporting Information, Sections 2.7 and 2.8). Compounds **4a** and **4b** show broad  $^{45}Sc$  NMR signals at  $\delta=451$  and 443 ppm (Figures S27 and S31), respectively, which appear markedly downfield shifted compared to the value observed for the corresponding reduced anthracene complex **3-Anth-K** ( $\delta=364$  ppm).

Protonation of **3-Anth-Li** with one equivalent of  $[NEt_3H][BPh_4]$  in THF resulted in an immediate color change from bright-red to light-orange. A  $^1H$  NMR spectrum of the crude reaction mixture confirmed the selective formation of the mono-protonated product  $[Sc(C_{14}H_{11})\{N(tBu)(Xy)\}_2(thf)]$  (**5**) along with  $[LiBPh_4]$  as a byproduct (Scheme 3). Further protonation of compound **5** led to the formation of 9,10-dihydroanthracene. After workup and crystallization, the mono-protonated product was isolated as an analytically pure off-white solid in 70% yield (see the Supporting Information, Section 2.9). Compound **5** is a thermally stable solid but decomposes instantaneously upon exposure to air.

The molecular structure of compound **5** was confirmed by single-crystal X-ray diffraction (Figure 5), which revealed a distorted tetrahedral geometry around the scandium center. Unlike the reduced arene complexes **3-Anth-M** ( $M=Li, Na, \text{ and } K$ ), the mono-anionic, protonated anthracene ligand in **5** is

bound in  $\eta^1$ -fashion. Whereas the Sc–C<sub>Anth</sub> bond length in **5** remains nearly the same (2.333(3) (**5**) vs. 2.358(3) Å (**3-Anth-Li**)), protonation of the reduced arene ligand resulted in a significant shortening of the Sc–N bonds ( $d(Sc-N)_{avg}=2.02$  (**5**) vs. 2.13 Å (**3-Anth-Li**)), indicating an increased back-donation from  $N \rightarrow Sc$  in the protonated complex.

The solution NMR spectra of compound **5** in  $[D_6]$ benzene corroborates the solid-state structure and confirms  $C_s$  symmetry in solution. The most notable spectroscopic feature of **5** is the  $^{45}Sc$  NMR signal at  $\delta=461$  ppm, which is markedly upfield shifted compared to those of the reduced arene complexes (Figure 2).

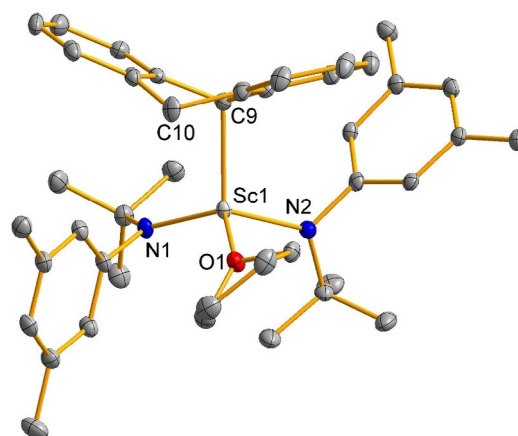


**Figure 5.** Molecular structure of **5** in the solid state with displacement parameters at 30% probability level. Hydrogen atoms are omitted for clarity. Selected interatomic distances (Å) and angles (°): Sc1–N1 2.017(3), Sc1–N2 2.027(3), Sc1–O1 2.141(2), Sc1–C9 2.333(3); N1–Sc1–N2 113.75(11), O1–Sc1–N1 118.28(9), O1–Sc1–N2 100.81(10), N1–Sc1–C9 108.57(11), N2–Sc1–C9 108.52(11), O1–Sc1–C9 106.26(11).

## Conclusions

In conclusion, scandium complexes of reduced naphthalene (**3-Naph-K**) and anthracene (**3-Anth-M**;  $M=Li, Na, \text{ and } K$ ) ligands can be classified as  $[ScX_n]^-$ -type “ate” complexes of trivalent scandium rather than scandium(I) complexes of  $[Sc(L)_xX_2]^-$  type. The molecular structures of the anthracene complexes reveal that the potassium complex forms a contact ion pair through coordination with the anthracene dianion, whereas the lithium and sodium analogues form solvent-separated ion pairs. The anthracene dianion is coordinated to the scandium center in a  $\sigma^2$ -bonding fashion. Quantum chemical calculations confirm that both complexes are present in the singlet state with a scandium(III) center with the naphthalene or the anthracene dianion. Aryl and alkyl nitriles insert into one of the two  $\sigma$  bonds of the anthracenide ligand to give metallocyclic compounds of scandium(III), as benzonitrile inserts into a Sc–diene bonds.<sup>[22]</sup> Reaction of the “ate” complex **3-Anth-Li** with one equivalent of a proton source led to selective protonation of the anthracene dianion under formation of an anthracene monoanion.

## Experimental Section

**Crystallographic data:** Deposition numbers 1968754, 1968755, 1968756, 1968757, 1968758, 1968759, 1972178, 1972179, and 1983913 contain the supplementary crystallographic data for this paper. These data are provided free of charge by the joint Cambridge Crystallographic Data Centre and Fachinformationszentrum Karlsruhe Access Structures service.

## Acknowledgements

We thank the Deutsche Forschungsgemeinschaft for financial support, D. Tomczak for help with experimental work, F. Ritter for assistance with X-ray crystallography, F. Thomas for UV/Vis spectroscopy, Dr. G. Fink for NMR measurements, and Prof. Dr. S. Herres-Pawlis for helpful discussions. We furthermore thank the Paderborn Center for Parallel Computing, PC<sup>2</sup>, for providing computing time on the High Performance Computing (HPC) system OCuLUS as well as support. Open access funding enabled and organized by Projekt DEAL.

## Conflict of interest

The authors declare no conflict of interest.

**Keywords:** alkali metals · arenes · charge transfer · NMR spectroscopy · scandium · UV/Vis spectroscopy

- [1] a) R. Benken, H. Günther, *Helv. Chim. Acta* **1988**, *71*, 694; b) M. Yus, R. P. Herrera, A. Guijarro, *Tetrahedron Lett.* **2001**, *42*, 3455; c) C. Melero, A. Guijarro, M. Yus, *Dalton Trans.* **2009**, 1286; d) T. A. Scott, B. A. Ooro, D. J. Collins, M. Shatruk, A. Yakovenko, K. R. Dunbar, H.-C. Zhou, *Chem. Commun.* **2009**, 65; e) A. Uresk, N. J. O'Neil, Z. Zhou, Z. Wei, M. A. Petrukhina, *J. Organomet. Chem.* **2019**, *897*, 57.
- [2] a) R. G. Lawler, C. V. Ristagno, *J. Am. Chem. Soc.* **1969**, *91*, 1534; b) W. E. Rhine, J. Davis, G. Stucky, *J. Am. Chem. Soc.* **1975**, *97*, 2079; c) B. Bogdanović, S.-T. Liao, R. Mynott, K. Schlichte, U. Westeppe, *Chem. Ber.* **1984**, *117*, 1378; d) C. L. Raston, G. Salem, *J. Chem. Soc. Chem. Commun.* **1984**, 1702; e) B. Bogdanović, N. Janke, C. Krüger, R. Mynott, K. Schlichte, U. Westeppe, *Angew. Chem. Int. Ed. Engl.* **1985**, *24*, 960; *Angew. Chem.* **1985**, *97*, 972; f) L. M. Engelhardt, S. Harvey, C. L. Raston, A. H. White, *J. Organomet. Chem.* **1988**, *341*, 39; g) M. Nir, I. O. Shapiro, R. E. Hoffman, M. Rabinovitz, *J. Chem. Soc. Perkin Trans. 2* **1996**, 1607.
- [3] a) B. Bogdanović, *Angew. Chem. Int. Ed. Engl.* **1985**, *24*, 262; *Angew. Chem.* **1985**, *97*, 253; b) C. Schöttle, P. Bockstaller, R. Popescu, D. Gerthsen, C. Feldmann, *Angew. Chem. Int. Ed.* **2015**, *54*, 9866; *Angew. Chem.* **2015**, *127*, 10004; c) C. Schöttle, D. E. Doronkin, R. Popescu, D. Gerthsen, J.-D. Grunwaldt, C. Feldmann, *Chem. Commun.* **2016**, *52*, 6316.
- [4] a) N. S. Poonia, A. V. Bajaj, *Chem. Rev.* **1979**, *79*, 389; b) M. D. Fryzuk, L. Jafarpour, F. M. Kerton, J. B. Love, S. J. Rettig, *Angew. Chem. Int. Ed.* **2000**, *39*, 767; *Angew. Chem.* **2000**, *112*, 783; c) G. K. Fukin, S. V. Lindeman, J. K. Kochi, *J. Am. Chem. Soc.* **2002**, *124*, 8329.
- [5] a) A. Minsky, A. Y. Meyer, R. Poupko, M. Rabinovitz, *J. Am. Chem. Soc.* **1983**, *105*, 2164; b) R. J. Bushby, H. L. Steel, *J. Chem. Soc. Perkin Trans. 2* **1990**, 1169; c) W. Huang, F. Dulong, T. Wu, S. I. Khan, J. T. Miller, T. Cantat, P. L. Diaconescu, *Nat. Commun.* **2013**, *4*, 1448.
- [6] a) W. W. Brennessel, J. Young, G. Victor, J. E. Ellis, *Angew. Chem. Int. Ed.* **2002**, *41*, 1211; *Angew. Chem.* **2002**, *114*, 1259; b) J. E. Ellis, *Inorg. Chem.* **2006**, *45*, 3167; c) R. E. Jilek, M. Jang, E. D. Smolensky, J. D. Britton, J. E. Ellis, *Angew. Chem. Int. Ed.* **2008**, *47*, 8692; *Angew. Chem.* **2008**, *120*, 8820; d) R. Wolf, E.-M. Schnöckelborg, *Chem. Commun.* **2010**, *46*, 2832; e) W. W. Brennessel, J. E. Ellis, *Inorg. Chem.* **2012**, *51*, 9076; f) Y. Nakanishi, Y. Ishida, H. Kawaguchi, *Dalton Trans.* **2016**, *45*, 15879; g) Y. Nakanishi, Y. Ishida, H. Kawaguchi, *Dalton Trans.* **2018**, *47*, 6903; h) J. E. Ellis, *Dalton Trans.* **2019**, *48*, 9538.
- [7] a) E.-M. Schnöckelborg, J. J. Weigand, R. Wolf, *Angew. Chem. Int. Ed.* **2011**, *50*, 6657; *Angew. Chem.* **2011**, *123*, 6787; b) W. Huang, P. L. Diaconescu, *Chem. Commun.* **2012**, *48*, 2216.
- [8] a) D. M. Roitershtein, A. M. Ellern, M. Y. Antipin, L. F. Rybakova, Y. T. Struchkov, E. S. Petrov, *Mendeleev Commun.* **1992**, *2*, 118; b) D. M. Roitershtein, L. F. Rybakova, E. S. Petrov, A. M. Ellern, M. Y. Antipin, Y. T. Struchkov, *J. Organomet. Chem.* **1993**, *460*, 39; c) I. L. Fedushkin, M. N. Bochkarev, S. Dechert, H. Schumann, *Chem. Eur. J.* **2001**, *7*, 3558; d) M. N. Bochkarev, *Chem. Rev.* **2002**, *102*, 2089; e) D. M. Roitershtein, A. V. Romanenkov, K. A. Lyssenko, P. A. Belyakov, M. Y. Antipin, *Russ. Chem. Bull.* **2007**, *56*, 1749.
- [9] W. Huang, S. I. Khan, P. L. Diaconescu, *J. Am. Chem. Soc.* **2011**, *133*, 10410.
- [10] J. L. Brosmer, W. Huang, P. L. Diaconescu, *Organometallics* **2017**, *36*, 4643.
- [11] J. E. Ellis, M. E. Minyaev, I. E. Nifant'ev, A. V. Churakov, *Acta Crystallogr. Sect. C* **2018**, *74*, 769.
- [12] a) J. S. Silvia, C. C. Cummins, *J. Am. Chem. Soc.* **2010**, *132*, 2169; b) A. F. Cozzolino, D. Tofan, C. C. Cummins, M. Temprado, T. D. Palluccio, E. V. Rybak-Akimova, S. Majumdar, X. Cai, B. Captain, C. D. Hoff, *J. Am. Chem. Soc.* **2012**, *134*, 18249; c) A. Paparo, J. S. Silvia, C. E. Kefalidis, T. P. Spaniol, L. Maron, J. Okuda, C. C. Cummins, *Angew. Chem. Int. Ed.* **2015**, *54*, 9115; *Angew. Chem.* **2015**, *127*, 9243; d) M.-A. Courtemanche, W. J. Transue, C. C. Cummins, *J. Am. Chem. Soc.* **2016**, *138*, 16220.
- [13] a) R. Anwander, O. Runte, J. Eppinger, G. Gerstberger, E. Herdtweck, M. Spiegler, *J. Chem. Soc. Dalton Trans.* **1998**, 847; b) T. Spallek, O. Heß, M. Meermann-Zimmermann, C. Meermann, M. G. Klimpel, F. Estler, D. Schneider, W. Scherer, M. Tafipolsky, K. W. Törnroos, C. Maichle-Mössmer, P. Sirsch, R. Anwander, *Dalton Trans.* **2016**, *45*, 13750; c) D. H. Woen, G. P. Chen, J. W. Ziller, T. J. Boyle, F. Furche, W. J. Evans, *Angew. Chem. Int. Ed.* **2017**, *56*, 2050; *Angew. Chem.* **2017**, *129*, 2082.
- [14] The degree of pyramidalization ranges between 0% for a trigonal-planar coordinated central atom and 100% for the sum of angles of 270°. The degree of pyramidalization was calculated as followed: % of pyramidalization =  $(360^\circ - \sum \angle \text{Sc}) / 90^\circ \times 100\%$ .
- [15] D. Barisic, D. Diether, C. Maichle-Mössmer, R. Anwander, *J. Am. Chem. Soc.* **2019**, *141*, 13931.
- [16] C. M. Kotyk, M. R. MacDonald, J. W. Ziller, W. J. Evans, *Organometallics* **2015**, *34*, 2287.
- [17] a) X. Min, I. A. Popov, F.-X. Pan, L.-J. Li, E. Matito, Z.-M. Sun, L.-S. Wang, A. I. Boldyrev, *Angew. Chem. Int. Ed.* **2016**, *55*, 5531; *Angew. Chem.* **2016**, *128*, 5621; b) D. H. Woen, G. P. Chen, J. W. Ziller, T. J. Boyle, F. Furche, W. J. Evans, *J. Am. Chem. Soc.* **2017**, *139*, 14861.
- [18] R. L. Martin, *J. Chem. Phys.* **2003**, *118*, 4775.
- [19] a) A. Schäfer, C. Huber, R. Ahlrichs, *J. Chem. Phys.* **1994**, *100*, 5829; b) V. N. Staroverov, G. E. Scuseria, J. Tao, J. P. Perdew, *J. Chem. Phys.* **2003**, *119*, 12129; c) J. Tao, J. P. Perdew, V. N. Staroverov, G. E. Scuseria, *Phys. Rev. Lett.* **2003**, *91*, 146401; d) V. N. Staroverov, G. E. Scuseria, J. Tao, J. P. Perdew, *J. Chem. Phys.* **2004**, *121*, 11507; e) F. Weigend, R. Ahlrichs, *Phys. Chem. Chem. Phys.* **2005**, *7*, 3297; f) L. Goerigk, S. Grimme, *Phys. Chem. Chem. Phys.* **2011**, *13*, 6670; g) S. Grimme, S. Ehrlich, L. Goerigk, *J. Comput. Chem.* **2011**, *32*, 1456; h) A. Hoffmann, R. Grunzke, S. Herres-Pawlis, *J. Comput. Chem.* **2014**, *35*, 1943.
- [20] a) F. Weinhold, C. Landis, *Valency and Bonding—A Natural Bond Orbital Donor–Acceptor Perspective*, Cambridge University Press, New York, **2005**; b) E. D. Glendening, J. K. Badenhop, A. E. Reed, J. E. Carpenter, J. A. Bohmann, C. M. Morales, C. R. Landis, F. Weinhold, Theoretical Chemistry Institute, University of Wisconsin, Madison, **2013**; c) E. D. Glendening, C. R. Landis, F. Weinhold, *J. Comput. Chem.* **2013**, *34*, 1429.
- [21] M. J. G. Lesley, M. R. Pineau, A. D. Hunter, M. Zeller, *Acta Crystallogr. Sect. E* **2004**, *60*, o1937.
- [22] D. J. Beetstra, A. Meetsma, B. Hessen, J. H. Teuben, *Organometallics* **2003**, *22*, 4372.
- [23] J.-P. Mazaleyrat, *Can. J. Chem.* **1978**, *56*, 2731.

Manuscript received: February 21, 2020

Accepted manuscript online: March 11, 2020

Version of record online: July 13, 2020